

# PROCEEDINGS OF SPIE REPRINT



SPIE—The International Society for Optical Engineering

*Reprinted from*

## ***Optical Remote Sensing of the Atmosphere and Clouds II***

9–12 October 2000  
Sendai, Japan



**Volume 4150**

# Stratospheric Background Aerosols and Polar Stratospheric Clouds Observed with Satellite Sensors - Inference of particle composition and sulfate amount -

S. Hayashida<sup>a</sup>, N. Saitoh<sup>a</sup>, M. Horikawa<sup>a</sup>, Y. Amemiya<sup>a</sup>, C. Brogniez<sup>b</sup>, T. Deshler<sup>c</sup>  
and Y. Sasano<sup>d</sup>

<sup>a</sup> Faculty of Science, Nara Women's University, Kita-uoya Nishi-machi,  
Nara 630-8506, Japan.

<sup>b</sup> Universite des Sciences et Technologies de Lille, 59655 Villeneuve d'Ascq Cedex, France.

<sup>c</sup> University of Wyoming, Laramie, WY, USA.

<sup>d</sup> National Institute for Environmental Studies, Onogawa 16-1, Tsukuba, Ibaraki 305, Japan

## ABSTRACT

The Improved Limb Atmospheric Spectrometer (ILAS) on board the Advanced Earth Observing Satellite (ADEOS) successfully observed atmospheric profiles over the Arctic and Antarctic from November 1996 through June 1997. It revealed the frequent occurrence of Polar Stratospheric Clouds (PSCs) over the Arctic between January and mid-March 1997. The ILAS provides a unique data set, including aerosol extinction at 780 nm, nitric acid, water vapor, and nitrous oxide, simultaneously. This paper demonstrates the validity of the ILAS aerosol data and presents an approach to estimate the chemical composition of PSCs. Comparisons are made with data from the Stratospheric Aerosol and Gas Experiment (SAGE) II.

**Keywords:** ILAS, Satellite, Stratospheric aerosol, Stratospheric Ozone, PSCs

## 1. INTRODUCTION

The Improved Limb Atmospheric Spectrometer (ILAS) is onboard the Advanced Earth Observing Satellite (ADEOS), which was launched in August 1996; regular operations started in November 1996.<sup>1-5</sup> ILAS is an occultation sensor designed to monitor, at 1-km height intervals, ozone (O<sub>3</sub>) and ozone-related species including PSC-related aerosols, nitric acid (HNO<sub>3</sub>), nitrogen dioxide (NO<sub>2</sub>), nitrous oxide (N<sub>2</sub>O), methane (CH<sub>4</sub>), and water vapor (H<sub>2</sub>O). ILAS made daily observations in both hemispheres at 14 points around the poles (57.1°-72.7°N and 64.3°-88.2°S). (See Sasano et al., Figure 1).<sup>2</sup> The ILAS provided measurements from November 1996 through June 1997. It was the only space-borne sensor that regularly monitored Arctic PSCs during the 1996/1997 winter, when significant ozone loss was observed over the Arctic<sup>6</sup> and PSCs frequently appeared.<sup>7</sup>

Analysis of the ILAS ozone data<sup>4</sup> showed a maximum ozone loss on the 450 K isentropic surface in the latter half of February at a rate of 84 +/- 17 ppbv/day. Significant ozone loss is well correlated with PSCs. Using a chemical box model along trajectories, Kagawa and Hayashida<sup>8</sup> recently suggested a link between heterogeneous reactions on the PSC surfaces and ozone loss. The amount of ozone lost via the chemical reaction depends on the rate of heterogeneous reactions and the amount of nitric acid in the atmosphere. Therefore, the chemical composition of the PSC aerosols is of scientific interest. Santee et al.<sup>9</sup> analyzed nitric acid data observed by MLS (Microwave Limb Sounder) and discussed the chemical compositions of PSCs. Saitoh et al.<sup>10</sup> analyzed the ILAS aerosol and nitric acid data and found several different types of PSCs. This paper addresses the validity of the ILAS aerosol data and discusses a method to estimate the amount of sulfates in the polar stratosphere with an approach that characterizes STS (supercooled ternary solution) particles.

---

Send correspondence to S. Hayashida  
S. Hayashida: sachiko@ics.nara-wu.ac.jp  
Y. Sasano: sasano@nies.go.jp

## 2. ILAS VERSION 4.20 DATA

### 2.1. ILAS Instrument and Aerosol Retrieval Algorithm version 4.20

The ILAS has two spectrometers: a 44-channel infrared (IR) spectrometer, that senses from 6.21 to 11.76 microns ( $850\text{-}1610\text{ cm}^{-1}$ ), and a 1024-channel near-visible spectrometer that senses at wavelengths 753 to 784 nm. This study shows results from the ILAS version 4.20 data; the data processing algorithm has been described in the Appendix of Hayashida et al.<sup>7</sup> in detail.

### 2.2. Kiruna balloon campaign - Validation and PSC appearances over the Arctic

Several field experiments were conducted to obtain validation data for the ILAS. One of the major experiments was conducted near Kiruna, Sweden, at Esrange (67.9°N, 21.1°E), from February through March 1997, in cooperation with the Centre National d'Etudes Spatiales (CNES). Table 1 lists the balloon-borne aerosol measurements that were made at Kiruna. Kanzawa et al.<sup>11</sup> provide an overview of the entire Kiruna experiment.

**Table 1.** Balloon-borne aerosol validation experiments and ILAS measurements at geographically closest locations OPC measurements(PI:T.Deshler)

OPCsite	OPC and ILAS data	OPC time(UT)	lat.,lon.	ILAS time(UT)	lat.,lon.	distance	time difference	comment
Andoya	1997.01.19	15:45	69.3N 16.0E	13:07	65.7N 21.3E	459.5km	2:38	PSC 18-25 km
Kiruna	1997.02.10	09:11	67.9N 21.1E	14:56	68.3N 10.3E	451.7km	5:45	
Kiruna	1997.02.11	09:25	67.9N 21.1E	14:29	68.4N 17.9E	141.6km	5:04	
Kiruna	1997.02.23	19:49	67.9N 21.1E	15:47	69.3N 10.0E	475km	4:02	PSC 18-21km small balloon
Kiruna	1997.02.25	09:16	67.9N 21.1E	14:52	69.4N 25.6E	249.1km	5:36	16-22 large particles : source unknown, T warm

RADIBAL measurement (PI: C. Brogniez)

RADIBAL site	RADIBAL and ILAS date	RADIBAL time (UT)	lat., lon.	ILAS time (UT)	lat., lon.	distance	time difference
Kiruna	1997.02.09	07:30	67.9N, 21.1E	13:43	68.2N, 27.8E	278.5km	6:13

\* Time of validation experiment is based on the launch time of balloon and ILAS time is based on the lowest altitude measurement.

One set of measurements was achieved using a RADIBAL, a photo-polarimeter that measures, at two near-infrared wavelengths (850 and 1650 nm), the radiance and the degree of polarization of sunlight scattered by the atmosphere at various scattering angles.<sup>12</sup> Comparison of these measured data with data from Mie computations produced an aerosol size distribution from which the extinction coefficient at 780 nm is derived. Figure 1 (left panel) shows a comparison of RADIBAL and ILAS extinction profiles: The two profiles are quite similar. A comparison of the two profiles is displayed in the right panel and shows good agreement, possibly because the methodology of RADIBAL measurements is similar to the satellite occultation measurements. In addition, the locations of the two measurements were reasonably close (278.5-km separation).

Five measurements of an Optical Particle Counter (OPC): one in January at Andoya, Norway (69.3°N, 16.0°E) and four in February at Kiruna, Sweden. The optical counter includes a white light source and a detector that is sensitive to light forward-scattered by particles. The magnitude of output pulses from the detector are observed in 12 channels, which correspond to particle radii larger than 0.15, 0.25, 0.30, 0.50, 0.75, 1.08, 1.25, 1.75, 2.50, 3.50, 5.00, and 10.00 micron, respectively. To determine the total aerosol population,  $r > 0.01$  micron, a second optical instrument is used that includes a growth chamber attached to the inlet. The condensation nuclei (CN) radii measured by this instrument are used when fitting size distributions to the aerosol measurements. The output pulses are counted; the cumulative number of particles at each size is sampled at 50-m intervals. These measurements are then averaged over 0.5 km and fitted with a log-normal size distribution.<sup>13</sup> Uncertainties of +/-30% are estimated for integrated distributions due to counting statistics and uncertainties in particle index of refraction.<sup>14</sup>

Comparisons of OPC measurements with ILAS 780 nm extinction data were achieved after Mie theory was applied to the OPC size distribution function to calculate a 780 nm extinction coefficient for OPC measurements. A refractive index of 1.43 and an imaginary part of zero was used in these computations. OPC data and the geographically nearest ILAS data were consistent on February 10, 1997 (Figure 2) but not on other days, because of PSC appearances over Kiruna. As shown in Table 1, PSCs were found by OPC at 18-25 km over Andoya on January 19 and at 18-21 km over Kiruna on February 23. The ILAS, however, observed PSC events more frequently over Northern Europe in January and February.<sup>7</sup>

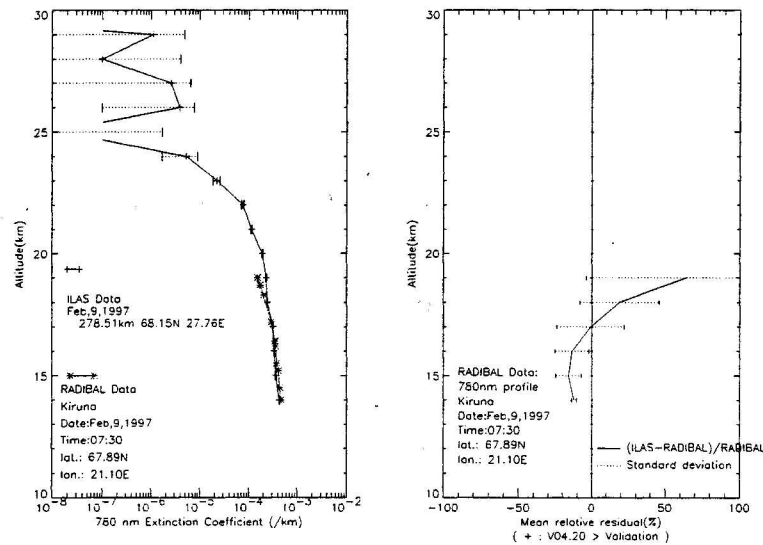


Figure 1. Comparison of ILAS with RADIBAL on February 9, 1997. (left) Comparison of profiles. (right) Relative difference.

To examine the inhomogeneity of aerosol distributions more closely, we compared all balloon data to any ILAS profile made within 24 hours and 1500 km of the balloon measurements. Table 2 is a list of the pair at most similar potential vorticity.

Table 2. List of the pair at most similar potential vorticity

OPC measurements(PI:T.Deshler)

OPCsite	OPC and ILAS data	OPC time(UT)	lat.,lon.	ILAS time(UT)	lat.,lon.	distance	PV( $10^{-6} m^2 K s^{-1} kg^{-1}$ ) difference
Andoya	1997.01.19	15:45	69.3N 16.0E	Jan.18,11:54	65.6N 39.1E	1061.8km	2.5
Kiruna	1997.02.10	09:11	67.9N 21.1E	Feb.10,13:15	68.3N 35.4E	594.5km	1.1
Kiruna	1997.02.11	09:25	67.9N 21.1E	Feb.12,14:02	68.5N 25.6E	195.5km	1.87
Kiruna	1997.02.23	19:49	67.9N 21.1E	Feb.24,17:00	69.4N 7.3W	1152km	1.83
Kiruna	1997.02.25	09:16	67.9N 21.1E	Feb.26,12:44	69.5N 58.6E	1500km	1.83

RADIBAL measurement (PI: C. Brogniez)

RADIBAL site	RADIBAL and ILAS date	RADIBAL time (UT)	lat., lon.	ILAS time (UT)	lat., lon.	distance	PV( $10^{-6} m^2 K s^{-1} kg^{-1}$ ) difference
Kiruna	1997.02.09	07:30	67.9N, 21.1E	13:43	68.2N,27.8E	278.5km	1.1

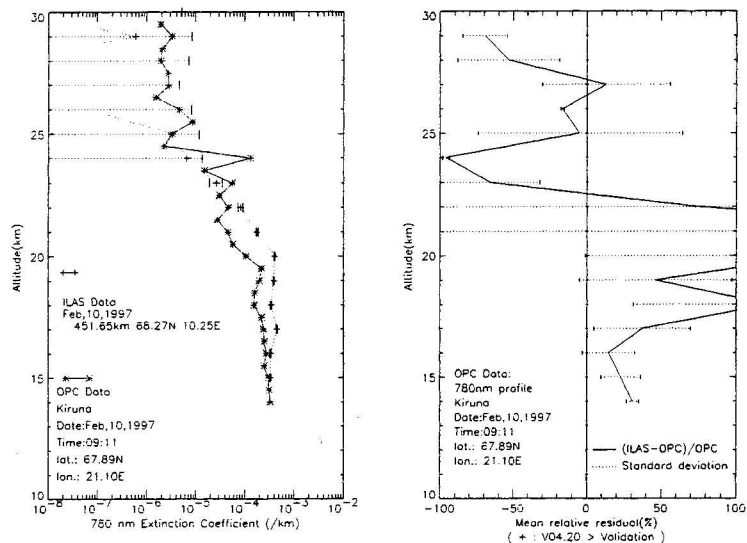


**Figure 2.** Comparison of ILAS with OPC on February 10, 1997. (left) Comparison of profiles. (right) Relative difference.

Figure 3 (left) shows scatterplots of the extinction values derived from RADIBAL and the ILAS measurements on February 9, and Figure 3 (right) shows the same but for OPC/ILAS comparison on February 10. Crosses indicate the pairs of data that are nearest geographically; squares correspond to locations with the most similar potential vorticity. The correlation between the two data sets is better for the pairs with similar vorticity. As shown in Figure 3 (right) PSC events (circles) are not well correlated because of the inhomogeneity of PSC distribution, and different sampling volumes in the instruments. Figure 4 shows an example of PSC event observed with OPC on January 19. The extinction derived from OPC and ILAS at geographically nearest location are not consistent, because OPC observed PSC event and ILAS observed the background aerosol.

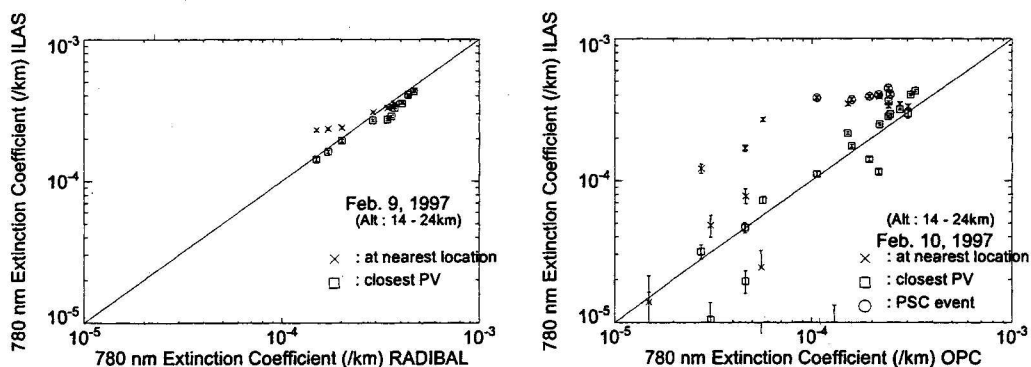


**Figure 3.** Scatter-plot of validation vs. ILAS data. (left) Correlation of RADIBAL and ILAS data on February 9, 1997 for the pair of geographically closest (crosses) and at most similar potential vorticity (square). Error bars are also indicated in the figure. (right) Correlation of OPC and ILAS data on February 10, 1997. PSC events are shown with open circles.

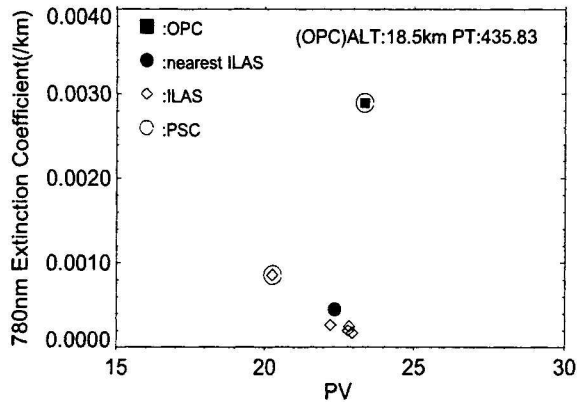


**Figure 4.** The extinction coefficients derived from OPC and ILAS data at 18.5km altitude on January 19, 1997 are plotted along potential vorticity (in PV unit). The OPC value is shown with the black rectangular, and the geographically nearest ILAS is shown with solid circle. The other ILAS data within 24 hours and 1500 km of the OPC measurement are shown with diamonds. PSC events are shown with open circles.

### 2.3. Comparison with SAGE II

Burton et al.<sup>15</sup> compared 73 pairs of nearly coincident profiles of aerosol extinction in the Southern Hemisphere. The profiles were produced for 1 week in January and February 1997 using ILAS version 3.10 and Stratospheric Aerosol and Gas Experiment (SAGE) II version 5.931. These profiles agree to within 10% for altitudes from approximately 15 to 24 km, although a small systematic bias at higher altitudes is evident. Hayashida et al.<sup>7</sup> showed that using ILAS version 4.20 resulted in very good agreement with the SAGE II profiles. SAGE II extinction coefficients at 525 nm and 1020 nm were logarithmically interpolated to 780 nm. Figure 5 shows these interpolated 780 nm extinction coefficients compared to ILAS 780 nm extinction coefficient profiles. Horizontal bars denote the first standard deviation of each. The comparison highlights the accuracy of ILAS version 4.20 aerosol data. In the figure, SAGE II extinction data at 1020-nm and 525-nm are also shown. The wavelength dependence of extinction (Ångström parameter) can be used to estimate a size distribution function. This will be discussed later.

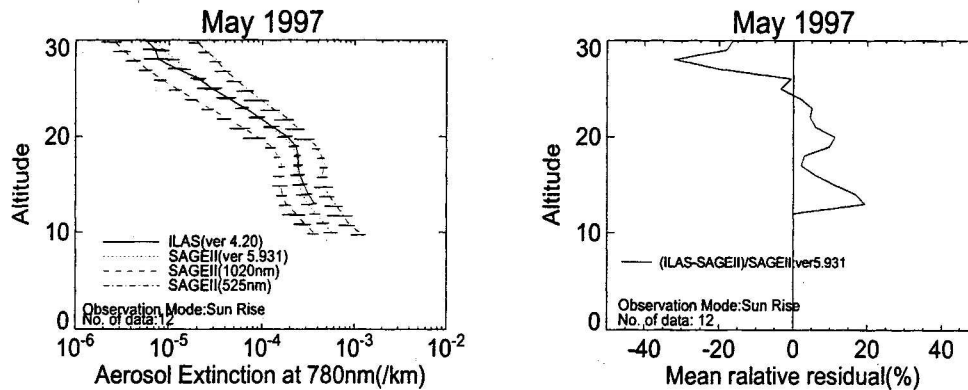


**Figure 5.** Comparison of the 780-nm extinction profiles observed with the ILAS and SAGE II. SAGE II extinction at 780 nm was derived by logarithmic interpolation of the extinction at 525 nm and 1020 nm.



### 3. POLAR STRATOSPHERIC CLOUDS OBSERVED WITH ILAS

#### 3.1. PSC appearance

Hayashida et al.<sup>7</sup> reported that the ILAS observed about 60 PSC profiles during the winter of 1996/1997 over the Arctic. Figure 6 shows the locations of PSC events observed in January through March 1997. The locations of PSC events in March is displaced to the east (to approximately 120°E) corresponding to a displacement of the polar vortex. In addition, the altitudes of PSC events in March decreased to about 18 km as a result of the cold air mass being displaced.

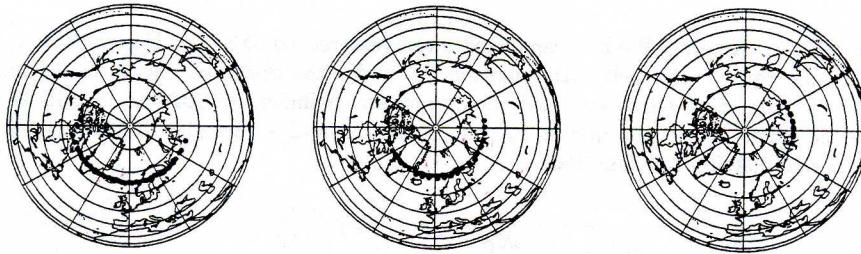


Figure 6. Maps of PSC events (from left) in January, in February and in March, 1997.

#### 3.2. Method to Characterize the Supercooled Ternary Solution (STS) particles

The ILAS provides a unique data set including 780 nm aerosol extinction, nitric acid, and water vapor simultaneously, all of which can be used to estimate the chemical composition of PSCs. A theoretical prediction of the volume of STS (Supercooled Ternary Solution) particles can be derived, based on an analytic expression of the thermodynamic equations as developed by Carslaw et al.<sup>16</sup> The volume and composition of ternary aerosols, as well as gaseous nitric acid in concentration at the specified temperature, can be calculated.

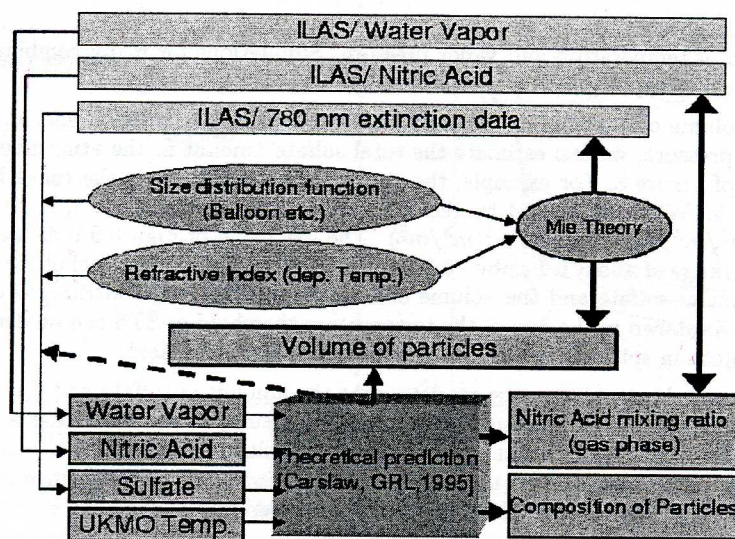


Figure 7. Schematic diagram to estimate STS particle volume by utilizing the thermodynamic model developed by Carslaw et al.<sup>16</sup> combined with ILAS data.

Figure 7 is a schematic diagram showing how the volume of STS particles is estimated using ILAS data. The ILAS measured nitric acid and water vapor as well as the aerosol extinction, thus we can use the data to estimate STS particle volume. Mie theory was applied to convert the ILAS 780 nm extinction into a volume using a refractive index that depends on temperature.<sup>17,18</sup> The size distribution functions were determined using the climatology of the Ångström parameter and the extinction coefficients derived from the SAGE II data set. As shown in Figure 4, the ILAS 780 nm extinction data are consistent with the interpolated SAGE II data, because the wavelength difference follows the relation,

$$\sigma = \sigma_0 \lambda^{-\alpha} \quad (1)$$

where  $\alpha$  is an Ångström parameter. We have analyzed a ten-year record of SAGE II global data, and found that the wavelength dependence agrees very well with equation (1) under the observed background conditions.<sup>19</sup> The climatological value of the Ångström parameter and the extinction coefficient of 1020 nm SAGE II data were used to determine the possible range of the parameters  $r_m$  (mode radius) and  $s$  (the distribution width), which can be expressed as log-normal size distribution function;

$$\frac{dn(r)}{dr} = \frac{N_0}{\sqrt{2\pi r \ln s}} \exp\left\{-\frac{\ln^2\left(\frac{r}{r_m}\right)}{2 \ln^2 s}\right\} \quad (2)$$

The derived size distribution parameters ( $r_m$  and  $s$ ) are used to convert the extinction into volume. Figure 8 shows the profile of the conversion factors derived from SAGE II data at 60°-70°N in March 1998. The conversion factors in Figure 8 are multiplied by the extinction ( $\text{km}^{-1}$ ) to yield the volume of particles. Carslaw's analytic solution<sup>16</sup> can also be used for binary conditions (sulfuric acid and water) under warm temperatures, yielding the relation between the total sulfate and the volume of binary particles expected at thermodynamic equilibrium. Figure 9 (left) shows the relation between the total amount of sulfate at thermodynamic equilibrium when the initial partial pressure of water vapor (i.e., vapor pressure) is 4 ppmv at 50 hpa ( $2 \times 10^{-4}$  hpa) and the temperature is 220 K. As shown in the figure, the expected volume of a particle is proportional to the total amount of sulfate when enough water vapor is available.<sup>20</sup> The relation between the total amount of sulfate ( $X$ ) and volume of particles ( $Y$ ) should be:

$$Y = aX \quad (3)$$

where  $a$  is a function of temperature and vapor pressure. Simulations for many combinations of values of temperature, pressure, and water vapor give the coefficient  $a$  for all possible conditions.

Once we know the volume of particles determined using the observed extinction and a specified combination of temperature and vapor pressure, we can estimate the total sulfate amount in the atmosphere using the relation as shown in the left panel of Figure 8. For example, the extinction at 780 nm is in the range between  $1.5 \times 10^{-4}$  and  $2.0 \times 10^{-4}$  from Figure 5. When multiplied by the conversion factor from Figure 8, it gives the range of volume between  $3.75 \times 10^{-14} (\text{m}^3/\text{m}^3)$  and  $1.0 \times 10^{-14} (\text{m}^3/\text{m}^3)$ . The left panel of Figure 9 indicates it is connected to the sulfate amount is in the range of about 0.1 ppbv - 0.5 ppbv at 50 hpa. The right panel of Figure 9 shows the relation between the total amount of sulfate and the volume of ternary particles if the nitric acid concentration is 6 ppbv and 12 ppbv at 50 hpa. As shown in the figure, the temperature threshold of STS can be determined with relatively narrow range of uncertainty in spite of the uncertainties of sulfate and nitric acid.

In the same manner with binary case, once we determine the amount of sulfate and the volume of STS particles (or gaseous nitric acid remaining in the atmosphere) at low temperature, we can derive the total amount of nitric acid that must have existed before STS formation. However, the difficulty in determining the size distribution function for PSCs prevents us from following the same procedure as for binary particles. Instead, we use the background average of nitric acid data observed by the ILAS for each 10-day period.

### 3.3. Examples of STS particles observed in January 1997

All the ILAS nitric acid and aerosol profiles were compared with theoretically predicted values of STS in a collocated UKMO temperature. Figure 10 (left) is a scatterplot of the extinction versus temperature in mid-January 1997 at 23 km. The solid circles in the figure correspond to extinction values beyond the threshold of PSC identification.<sup>7</sup> The



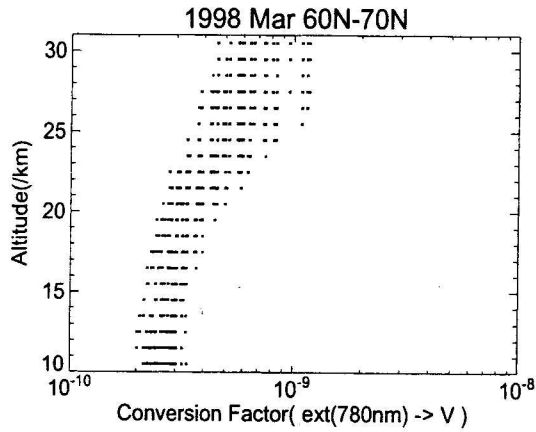


**Figure 8.** The factors to convert the extinction coefficient ( $\text{km}^{-1}$ ) into volume ( $\text{m}^3/\text{m}^3$ ) for background sulfate aerosols derived from SAGE II data in March 1998 at  $60^\circ$ - $70^\circ\text{N}$ .

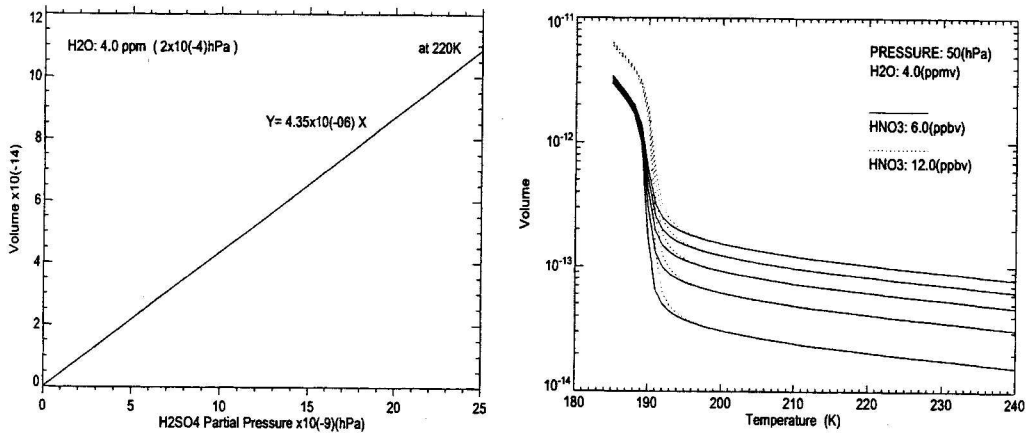


**Figure 9.** (left) Linear relation between the total sulfate amount in the atmosphere and the volume of binary aerosol particles under thermodynamic equilibrium. (right) Relation between the total sulfate and the volume of STS (supercooled ternary solution) particles.

particle formation curve for STS is also shown (volume was concentrated to the extinction by the conversion factor). PSC data observed over the Arctic in 1997 show good correspondence to theoretically predicted values, suggesting particle growth of STS at low temperature. The right panel of Figure 10 shows that nitric acid also decreased, agreeing with theoretical predictions of STS particle formation. Figure 11 shows the profile of a PSC observed on January 20, 1997. The theoretical simulation above predicts the enhancement of particle volume concomitant with the apparent decrease in nitric acid. The formation of STS is also suggested in the figure, although there are significant quantitative discrepancies. However, other PSC observations over the Arctic in 1997 do show good correspondence to theoretically predicted values, suggesting particle growth of STS at low temperature. NAT (Nitric Acid Trihydrate) and NAD (Nitric Acid Dihydrate) particle formation can be also investigated using the ILAS nitric acid and water vapor data.<sup>10</sup> The details of these particle formations are now under study.

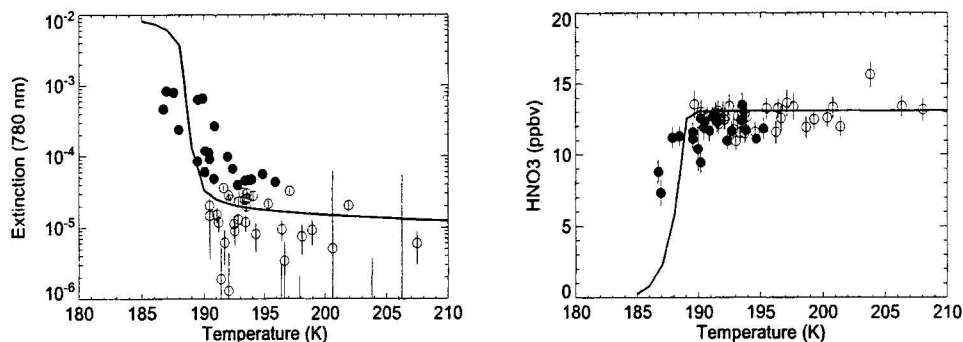


**Figure 10.** (left) Scatterplot of the extinction and temperature observed at 23-km altitude in mid-January, 1997. (right) Scatterplot of the nitric acid and temperature corresponding to the left panel.

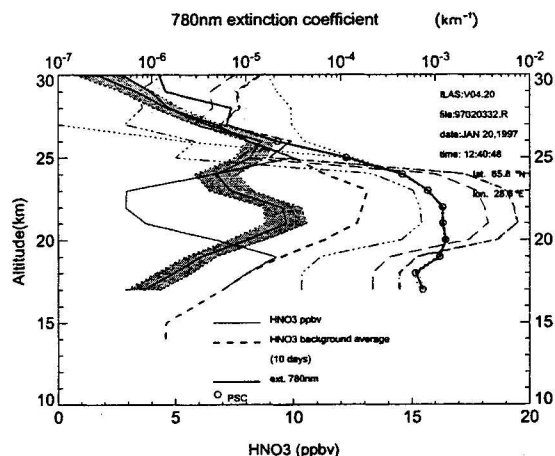


**Figure 11.** A typical example of STS profiles observed on January 20, 1997 with theoretically predicted values. Thick solid line with circles (upper scale) : the profile of extinction at 780nm. Circles are PSC events. Uncertainties are shown with gray shadow. Solid line with shadow : Profile of nitric acid (lower scale) with the range of uncertainty. Dashed line: Profile of the background average of nitric acid. Thin solid line: Simulated nitric acid after STS formation. Dashed and dotted lines : The profiles of extinction simulated as STS formation.

#### 4. SUMMARY

Aerosol extinction data at 780 nm, using the ILAS version 4.20, were validated and used to investigate the chemistry of Polar Stratospheric Clouds. A comparison with SAGE II data demonstrated the validity and reliability of the

ILAS aerosol data. Arctic aerosol data were closely analyzed for the winter 1996/1997, when a significant ozone decrease was observed. The ILAS observed active PSC occurrence in mid-January at approximately 23 km, followed by intermittent occurrence until mid-March, at approximately 18 km. The ILAS provides a unique data set including aerosol extinction at 780 nm, nitric acid, water vapor, and nitrous oxide, simultaneously. We used the thermodynamic model developed by Carslaw et al., to calculate the volume and composition of particles as well as the mixing ratio of gaseous nitric acid in gas phase at the observed temperature. We proposed a scheme to apply the ILAS data to a theoretical prediction of STS particle formation, and showed some representative data suggesting STS particle formation in mid-January 1997. A significant decrease in the mixing ratio was observed in some nitric acid profiles corresponding to intense PSC events, which suggests the uptake of gaseous nitric acid into particles.

### ACKNOWLEDGMENTS

We wish to express our great thanks to all of the ILAS science team members and their associates, and especially to Hiroshi Kanzawa (National Institute for Environmental Studies, Japan) for his efforts with the validation experiments, and to L. W. Thomason and S.P. Burton for their validation analysis with SAGE II data. We also thank to Ms Araki for her help in plotting figures. The ILAS retrieval data processing was carried out at the ILAS Data Handling Facility (DHF) at NIES. This study was partly supported by EORC/NASDA.

### REFERENCES

1. Y. Sasano, M. Suzuki, T. Yokota, and H. Kanzawa, "Improved Limb Atmospheric Spectrometer (ILAS) project:ILAS instrument, performance and validation plan," *J. Soc. Photo Opt. Instrum. Eng.* **2583**, pp. 193-204, 1995.
2. Y. Sasano, M. Suzuki, T. Yokota, and H. Kanzawa, "Improved Limb Atmospheric Spectrometer (ILAS) for stratospheric ozone layer measurements by solar occultation technique," *Geophys. Res. Lett.* **26**, pp. 197-200, 1999.
3. Y. Sasano, H. Nakajima, H. Kanzawa, M. Suzuki, T. Yokota, H. Nakane, H. Gernandt, A. Schmidt, A. Herber, V. Yushkov, V. Dorokhov, and T. Deshler, "Validation of ILAS version 3.10 ozone with ozonesonde measurements," *Geophys. Res. Lett.* **26**, pp. 831-834, 1999.
4. Y. Sasano, Y. Terao, H. L. Tanaka, T. Yasunari, H. Kanzawa, H. Nakajima, T. Yokota, H. Nakane, S. Hayashida, and N. Saitoh, "ILAS observations of chemical ozone loss in the Arctic vortex during early spring 1997," *Geophys. Res. Lett.* **27**, pp. 213-216, 2000.
5. T. Yokota, M. Suzuki, H. Kanzawa, H. Nakajima, and Y. Sasano, "ILAS data processing algorithm version 3.10," *Geophys. Res. Lett.* , 1998.
6. P. A. Newman, J. F. Gleason, R. D. McPeters, and S. R. Stolarski, "Anomalously low ozone over the Arctic," *Geophys. Res. Lett.* **24**, pp. 2689-2692, 1997.
7. S. Hayashida, N. Saitoh, A. Kagawa, T. Yokota, M. Susuki, H. Nakajima, and Y. Sasano, "Arctic polar stratospheric clouds observed with the Improved Limb Atmospheric Spectrometer during Winter 1996/1997," *J. Geophys. Res.* , 2000.
8. A. Kagawa and S. Hayashida, "Development of a chemical model of the polar regions," in *Quadrennial Ozone Symposium* , 2000.
9. M. L. Santee, A. Tabazadeh, G. L. Manney, R. J. Salawitch, L. Froidevaux, W. G. Read, and J. W. Waters, "UARS Microwave Limb Sounder HNO<sub>3</sub> observations: Implications for Antarctic polar stratospheric clouds," *J. Geophys. Res.* **103**, pp. 13285-13313, 1998.
10. N. Saitoh, S. Hayashida, H. Nakajima, and Y. Sasano, "Arctic PSCs observed with ILAS during the winter of 1996/1997: Analysis of temperature history and inference of the chemical composition of particles," in *Quadrennial Ozone Symposium* , pp. 621-622, 2000.
11. H. Kanzawa, C. Camy-Peyret, Y. Kondo, and N. Papineau, "European rocket and balloon programmes and related research," in *13th ESA Symp.* , pp. 211-215, 1997.
12. C. Brogniez, R. Santer, S. Diallo, M. Herman, J. Lenoble, and H. Jager, "Comparative observations of stratospheric aerosols by ground-based lidar, balloon-borne polarimeter and satellite solar occultation," *J. Geophys. Res.* **97**, pp. 20805-20823, 1992.
13. D. J. Hofmann and T. Deshler, "Stratospheric cloud observations during formation of the Antarctic ozone hole in 1989.," *J. Geophys. Res.* **96**, pp. 2897-2912, 1991.

14. A. E. Deshler, M. D. Burrage, J. U. Grooss, J. R. Holton, J. L. Lean, S. T. Massie, M. R. Schoeberl, A. R. Douglass, and C. H. Jackman, "Selected science highlights from the first 5 years of the Upper Atmosphere Research Satellite (UARS) program," *Reviews of Geophysics* **36**, pp. 183-210, 1998.
15. S. P. Burton, L. W. Thomason, Y. Sasano, and S. Hayashida, "Comparison of aerosol extinction measurements by ILAS and SAGEII," *Geophys. Res. Lett.* **26**, pp. 1719-1722, 1999.
16. K. S. Carslaw, S. L. Clegg, and P. Brimblecombe, "A thermodynamic model of the system HCL-HNO<sub>3</sub>-H<sub>2</sub>SO<sub>4</sub>-H<sub>2</sub>O, including solubilities of HBr, from < 200 to 328 K.," *J. Phys. Chem.* **99**, pp. 11,557-11,574, 1995.
17. B. Luo, U. K. Krieger, and T. Peter, "Densities and refractive indices of H<sub>2</sub>SO<sub>4</sub>/HNO<sub>3</sub>/H<sub>2</sub>O solutions to stratospheric temperatures.," *Geophys. Res. Lett.* **23**, pp. 3707-3710, 1996.
18. G. Beyerle, B. Luo, R. Neuber, T. Peter, and I. S. McDermid, "Temperature dependence of ternary solution particle volumes as observed by lidar in the Arctic stratosphere during winter 1992/1993.," *J. Geophys. Res.* **102**, pp. 3603-3609, 1997.
19. S. Hayashida and M. Horikawa, "Climatology of the Angstrom coefficient for stratospheric aerosols: background trend and volcanic," in *Quadrennial Ozone Symposium*, pp. 189-190, 2000.
20. H. M. Steele and P. Hamill, "Effects of temperature and humidity on the growth and optical properties of sulphuric acid-water droplets in the stratosphere," *J. Aerosol Sci.* **12**, pp. 517-528, 1981.